Analysis of double-β transitions in ^{78}Kr

Jouni Suhonen
Department of Physics, P. O. Box 35 (YFL), FI-40014 University of Jyväskylä, Finland
(Received 24 January 2013; published 20 March 2013)

In this paper a comprehensive theoretical analysis of the two-neutrino ($2\nu2\beta$) and neutrinoless ($0\nu2\beta$) double-beta decays of ^{78}Kr is performed by evaluating the corresponding nuclear matrix elements by combining the quasiparticle random-phase approximation with the multiple-commutator model. Transitions to the ground state $0^+_{\rm gs}$ and 0^+ and 2^+ excited states in ^{78}Se are investigated by using G-matrix-based nuclear forces. The channels $\beta^+\beta^+$, β^+EC, and ECEC are discussed for the $2\nu2\beta$ decays and the channels $\beta^+\beta^+$ and β^+EC for the $0\nu2\beta$ decays. The associated half-lives are computed to see if the detection of some of these transitions is experimentally feasible.

DOI: 10.1103/PhysRevC.87.034318 PACS number(s): 21.60.Jz, 23.40.Bw, 23.40.Hc, 27.50.+e

I. INTRODUCTION

At present we do not know whether the neutrino is a Majorana or Dirac particle or what is its absolute mass scale. On the other hand, neutrino-oscillation experiments have enabled precision measurements of the neutrino-oscillation parameters, including information on neutrino mixing and relative masses. It is well known that atomic nuclei can be of service in clarifying the fundamental nature of the neutrino by engaging the Majorana-neutrino-triggered neutrinoless double-beta ($0\nu2\beta$) decays. Here, the involved nuclear matrix elements (NMEs) constitute a long-debated issue [1–3] and their accurate evaluation is one of the most important challenges in present-day neutrino physics. It has become customary to harness the standard-model counterpart of the $0\nu2\beta$ decay; namely, the two-neutrino double-beta ($2\nu2\beta$) decay, to serve as a testing ground for the various nuclear models used in the NME calculations. This is feasible since $2\nu2\beta$-decay half-lives have been measured for several nuclei [4].

The positron-emitting modes of double-beta decays, $\beta^+\beta^+$, β^+EC [5,6] and ECEC [7–11] are much less studied than the double-β^- decays [2,3,12] owing to their less favorable decay Q values. Such decay modes could, however, be potentially interesting, as shown by several older studies [13–17] and some more recent ones [18–21]. In the present article the two-neutrino $\beta^+\beta^+$, β^+EC, and ECEC transitions and neutrinoless $\beta^+\beta^+$ and β^+EC transitions in ^{78}Kr are discussed. Considered are the transitions to the ground state $0^+_{\rm gs}$ and to the first- and second-excited 2^+ states 2^+_1 and 2^+_2, as well as to the first-excited 0^+ state 0^+_1 in the daughter nucleus ^{78}Se.

In this work the involved wave functions of the nuclear states are calculated by using the quasiparticle random-phase approximation (QRPA) in a realistically large single-particle model space (see Refs. [22–24] for a discussion of the model-space effects). In particular, the 2^+_1 state in ^{78}Se is assumed to be a one-phonon state of the charge-conserving QRPA (ccQRPA) [25], whereas the 0^+_1 and 2^+_2 states are assumed to consist of two 2^+_1 ccQRPA phonons as discussed in Refs. [23,24]. The J^π states of the intermediate nucleus ^{78}Br are treated by the proton-neutron QRPA (pnQRPA) [2,25]. The one- and two-phonon states in ^{78}Se are then connected to the J^π states of ^{78}Br by transition amplitudes obtained from a higher-QRPA framework called the multiple-commutator model (MCM), first introduced in Ref. [26] and further extended in Ref. [27]. For all the $0\nu2\beta$ transitions the NMEs are computed by the use of both the Jastrow short-range correlations [28] and the UCOM correlations [29,30]. Both short-range correlators have been recently used in many QRPA calculations [31–35] as also in shell-model calculations [36] and in some other calculations [37,38]. In addition, the contributions arising from the induced currents and the finite nucleon size [39] have been taken into account. The calculations of the present paper constitute an exhaustive treatment of the double-beta-decay properties of ^{78}Kr.

II. SHORT OUTLINE OF THEORETICAL FRAMEWORK

In this section only a short outline of the basic theoretical ingredients of the calculations is given. A more detailed presentation is given in a recent article [21].

In the presently discussed case of the ^{78}Kr two-neutrino double-beta decay $2\nu2\beta$, there are three different decay channels; namely, $\beta^+\beta^+$, β^+EC, and ECEC. The associated half-lives can be expressed as [1,5]

$$\left[T^{\alpha}_{2\nu}(I^+)\right]^{-1} = \frac{(Gg_{\rm A})^4 m_{\rm e}^9}{32\pi^7 \ln 2} \int dE^{(\alpha)} \mathcal{M}_\alpha(I^+), \qquad \alpha = \beta^+\beta^+,\ \beta^+{\rm EC},\ {\rm ECEC}, \tag{1}$$

where $I = 0, 2$ is the final-state angular momentum, G is the weak-interaction constant, $g_{\rm A}$ is the axial-vector coupling constant, $m_{\rm e}$ is the electron rest mass, and $\int dE^{(\alpha)}$ denotes integration over the lepton phase space. This integration is different for the different decay channels and leads to the following expressions for the half-lives [21]:

$$\left[T^{\beta^+\beta^+}_{2\nu}(I^+)\right]^{-1} = G^{\beta^+\beta^+}_{2\nu}(I^+)\left[M^{\beta^+\beta^+}_{2\nu}(I^+)\right]^2, \tag{2}$$

$$\left[T^{\beta^+{\rm EC}}_{2\nu}(I^+)\right]^{-1} = G^{\beta^+{\rm EC(K)}}_{2\nu}(I^+)\left[M^{\beta^+{\rm EC(K)}}_{2\nu}(I^+)\right]^2 + G^{\beta^+{\rm EC(L)}}_{2\nu}(I^+)\left[M^{\beta^+{\rm EC(L)}}_{2\nu}(I^+)\right]^2, \tag{3}$$

$$\left[T^{\rm ECEC}_{2\nu}(I^+)\right]^{-1} = G^{\rm EC(K)EC(K)}_{2\nu}(I^+)\left[M^{\rm EC(K)EC(K)}_{2\nu}(I^+)\right]^2 + G^{\rm EC(K)EC(L)}_{2\nu}(I^+)\left[M^{\rm EC(K)EC(L)}_{2\nu}(I^+)\right]^2, \tag{4}$$

where the expressions for the lepton phase-space integrals $G^{\alpha}_{2\nu}(I^+)$, $\alpha = \beta^+\beta^+,\ \beta^+\mathrm{EC},\ \mathrm{ECEC}$ are given in Ref. [5] and the NMEs $M^{\alpha}_{2\nu}(I^+)$ include the various energy denominators and a summation over all the 1^+ states of the intermediate nucleus ^{78}Br [21]. Above, the symbols EC(K) and EC(L) denote electron capture from the atomic K and L_1 shells, respectively.

For the $0\nu2\beta$ decays (via the exchange of a massive Majorana neutrino) the inverse half-lives for the $\beta^+\beta^+$ and β^+EC channels can be expressed in the form

$$\left[T^{\alpha}_{0\nu}(0^+)\right]^{-1} = G^{\alpha}_{0\nu}(0^+)|M^{(0\nu)'}|^2\,(|\langle m_\nu\rangle|[\mathrm{eV}])^2\,,$$
$$\alpha = \beta^+\beta^+,\ \beta^+\mathrm{EC}, \qquad (5)$$

where $\langle m_\nu\rangle$ is the effective neutrino mass [2] that should be given in Eq. (5) in units of eV. The phase-space integrals $G^{\beta^+\beta^+}_{0\nu}(0^+)$ and $G^{\beta^+\mathrm{EC}}_{0\nu}(0^+)$ are defined in Ref. [6]. The $0\nu2b$ NMEs are defined [22–24] in terms of the Gamow-Teller (GT), Fermi (F), and tensor (T) matrix elements

$$M^{(0\nu)'} = \left(\frac{g_{\mathrm{A}}}{1.25}\right)^2\left[M^{(0\nu)}_{\mathrm{GT}} - \left(\frac{g_{\mathrm{V}}}{g_{\mathrm{A}}}\right)^2 M^{(0\nu)}_{\mathrm{F}} + M^{(0\nu)}_{\mathrm{T}}\right], \qquad (6)$$

where $g_{\mathrm{A}} = 1.25$ corresponds to the bare-nucleon value of the axial-vector coupling constant and $g_{\mathrm{V}} = 1.00$ is the vector coupling constant. The tensor matrix element is neglected in the present calculations since its contribution is very small [31,36]. The Gamow-Teller and Fermi NMEs appearing in the half-life expressions are given in Ref. [21]. There also the involved one-body transition densities are written explicitly.

III. DETAILS OF MODEL CALCULATIONS

The single-particle space of the present nuclear-structure calculations contains the single-particle orbitals belonging to the $1p$-$0f$-$2s$-$1d$-$0g$-$0h_{11/2}$ shells for both protons and neutrons. The single-particle energies were first generated by the use of a global spherical Coulomb-corrected Woods-Saxon (WS) potential, defined in Ref. [40]. The BCS approximation was used to define the quasiparticles needed for the quasiparticle random-phase approximation (QRPA) calculations of the necessary wave functions in the intermediate nucleus ^{78}Br (proton-neutron form of the QRPA, pnQRPA [25]) and the final nucleus ^{78}Se (the like-particle form of the QRPA, denoted here as ccQRPA [21,25]). It turned out that the resulting energies of the one-quasiparticle states do not reproduce satisfactorily the low-energy spectra of the neighboring odd-A nuclei. This leads to manual adjustments of the WS energies for some key orbitals close to the proton and neutron Fermi surfaces. Adjustments of this spirit have been used on several occasions in past calculations (see, e.g., Refs. [22,24,35,41]). In the present case these adjustments also improved considerably the quality of the calculated beta-decay rates which served as a good check of the computed wave functions of the excited states in ^{78}Se. These decays will be discussed in detail in Sec. IV A.

The Bonn-A G-matrix has been used as the two-body interaction and it has been renormalized in the standard way [26,42]: the pairing matrix elements are scaled by a common factor, separately for protons and neutrons, and in practice these factors are fit such that the lowest quasiparticle energies obtained from the BCS match the experimental pairing gaps for protons and neutrons, respectively. The particle-hole and particle-particle parts of the proton-neutron two-body interaction are scaled by the particle-hole parameter g_{ph} and particle-particle parameter g_{pp}, respectively. The value of the particle-hole parameter, $g_{\mathrm{ph}} = 1.20$, was fixed by the available systematics [25] on the location of the Gamow-Teller giant resonance (GTGR) state.

The value of the g_{pp} parameter regulates the β^--decay amplitude of the first 1^+ state in the intermediate nucleus [43] and hence also the decay rates of the $\beta\beta$ decays. This value can be fixed either by the data on β^- decays [43] or by the data on $2\nu\beta^-\beta^-$-decay rates within the interval $g_{\mathrm{A}} = 1.00$–1.25 of the axial-vector coupling constant as done, e.g., in Refs. [30–32,34]. In the present case there are no data for the $2\nu\beta^-\beta^-$-decay rates and also no suitable data for the β^- decays. This poses a problem in an unambiguous selection of the physical values of g_{pp}. The only reasonable way to cope with the situation [35] is to choose a wide range of g_{pp} values in such a way that the largest adopted value does not bring the NME close to the collapse point of the pnQRPA. The lowest value of g_{pp} is chosen such that all the physically meaningful values of the $2\nu2\beta$ and $0\nu2\beta$ NMEs are safely covered. These procedures confine the values of the particle-particle parameter to the interval $g_{\mathrm{pp}} = 0.80$–1.05 in the present case.

For the ccQRPA the g_{ph} and g_{pp} parameters were fixed to the values $g_{\mathrm{ph}} = 0.582$ and $g_{\mathrm{pp}} = 1.00$ for the 2^+ channel. For the given value of g_{ph} the experimental location of the 2^+_1 state in ^{78}Se is reproduced by the ccQRPA calculations.

IV. RESULTS

In this section the main results of the present calculations are summarized. First the computed reduced half-lives, i.e., the $\log ft$ values, of several beta-decay transitions relevant for probing the wave functions in ^{78}Se are compared with the available $\log ft$ data. Second, various $2\nu2\beta$ and $0\nu2\beta$ observables are calculated for comparison with the possible future double-beta-decay experiments.

A. Single-β decays

The available data on β^--decay and β^+/EC-decay rates allow for studies of the lateral beta-decay feedings of the 0^+ ground state and low-lying excited 0^+, 2^+, and 4^+ states in the daughter nucleus ^{78}Se of the double-beta decay of ^{78}Kr. These states are shown in Fig. 1. From this figure one sees that the second 2^+ state 2^+_2, the first-excited 0^+ state 0^+_1, and the first 4^+ state 4^+_1 are all found at an energy roughly twice the energy of the first 2^+ state 2^+_1. This points to the vibrational nature of ^{78}Se and the possibility to treat the 2^+_2, 0^+_1, and 4^+_1 states as a two-phonon triplet based on the 2^+_1 state (see for further details in Ref. [24]).

In Fig. 1 is shown also the feeding of the indicated states by allowed Gamow-Teller β^+/EC transitions from ^{78}Br and first-forbidden β^- transitions from ^{78}As. In the figure the numbers

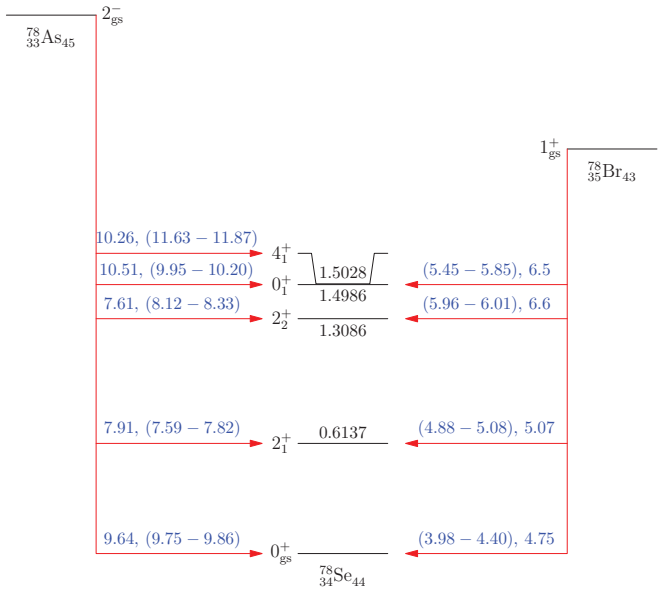

FIG. 1. (Color online) Level scheme of ^{78}Se and the feeding of the levels by allowed Gamow-Teller β^+/EC transitions from ^{78}Br and first-forbidden β^- transitions from ^{78}As. Given are the log ft values of the transitions with the computed ones (in parentheses) compared with the experimental ones.

are log ft values with the computed ones given as ranges in parentheses and the experimental ones as single numbers without parentheses. The computed numbers correspond to the range $g_A = 1.00$–1.25 for the axial-vector coupling constant translating to the interval $g_{pp} = 0.80$–1.05 for the particle-particle interaction strength parameter.

For the allowed β^+/EC decays of this work the log ft value is defined as [25]

$$\log ft = \log(f_0 t_{1/2}) = \log\left[\frac{6147}{B_{GT}}\right], \tag{7}$$

where the reduced Gamow-Teller transition probability is defined as

$$B_{GT} = \frac{g_A^2}{3}(J_f^+ \| \boldsymbol{\sigma} t^+ \| 1^+)^2 \tag{8}$$

for the initial 1^+ state in ^{78}Br and the final J_f^+ states in ^{78}Se. Here t^+ is the isospin raising operator and the vector $\boldsymbol{\sigma}$ contains the Pauli spin matrices. For the first-forbidden unique (FFU) β^- transitions $2^- \to 0^+$ and $2^- \to 4^+$ we can define [25]

$$\log ft = \log(f_{1u} t_{1/2}) = \log\left[\frac{6147}{\frac{1}{12} B_{1u}}\right],$$

$$B_{1u} = \frac{g_A^2}{2J_i + 1}\mathcal{M}_{1u}^2, \tag{9}$$

where

$$\mathcal{M}_{1u} = \frac{m_e c^2}{\sqrt{4\pi}}(J_f^+ \| [\boldsymbol{\sigma}\mathbf{r}]_2 t^- \| 2^-) \tag{10}$$

is for the initial 2^- and final $J_f^+ = 0^+, 4^+$ states. For the first-forbidden nonunique transitions $J_i^- \to J_f^+, |J_i - J_f| \leqslant 1$, we can define [25]

$$\log ft = \log(f_0 t_{1/2}) = \log\left[f_0 \frac{6147}{\mathcal{S}_1^{(-)}}\right], \tag{11}$$

where the shape function $\mathcal{S}_1^{(-)}$ can be inferred from Ref. [26].

From Fig. 1 one can see that the computed ranges of log ft values for the allowed Gamow-Teller β^+/EC transitions are generally somewhat low compared to the experimental values. This means by (7) that the computed decay rates are somewhat too fast. In the case of the first-forbidden β^- transitions the correspondence between the experimental and computed log ft values is satisfactory. It should be noted at this point that the computed figures of Fig. 1 refer to the adjusted single-particle basis discussed in Sec. III. The corresponding beta-decay results for the Woods-Saxon basis are much worse and thus give support to the single-particle-energy adjustments based on the analysis of the single-quasiparticle energies.

B. Two-neutrino double-β decays

Figure 2 summarizes the computed results for the $2\nu2\beta$ half-lives for different modes of decay, as deduced from Eqs. (2)–(4). From the figure one perceives that the decay mode $\beta^+\beta^+$ has a positive Q value (and thus can occur) only for the lowest-two final states. Instead, the ECEC and β^+EC modes are possible for all the final states of interest in this work. The ranges of decay half-lives are computed for the range $g_A = 1.00$–1.25 of the axial-vector coupling constant and correspond to the interval $g_{pp} = 0.80$–1.05 for the g_{pp} parameter. The absolute values of the involved NMEs are summarized in the last three columns of Table I where the first column gives the final state and the second column its interpretation either as the QRPA ground state (gs) or as a one-phonon state (1-ph) or a two-phonon state (2-ph). In the table the NMEs $M_{2\nu}^{\alpha}$ are those involved in Eqs. (2)–(4). The

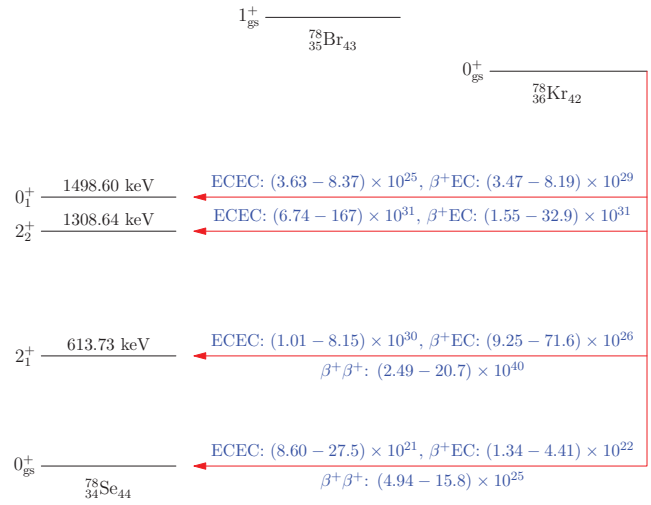

FIG. 2. (Color online) Computed partial decay half-lives of the ECEC, β^+EC, and $\beta^+\beta^+$ decay transitions from the ground state of ^{78}Kr to the ground and excited states in ^{78}Se. The half-lives are given in units of years.

TABLE I. Absolute values of the NMEs for the various $2\nu2\beta$ processes in ^{78}Kr. The first column gives the final state and the second column its interpretation either as the QRPA ground state (gs) or as a one-phonon state (1-ph) or a two-phonon state (2-ph). The last three columns give the absolute values of the NMEs $M^{\alpha}_{2\nu}$ involved in Eqs. (2)–(4).

Final state	Structure	$\lvert M^{\alpha}_{2\nu}\rvert$		
		ECEC	β^+EC	$\beta^+\beta^+$
$0^+_{\rm gs}$	gs	0.512 ± 0.223	0.532 ± 0.232	0.256 ± 0.111
2^+_1	1-ph	0.0017 ± 0.0012	0.0020 ± 0.0014	0.0014 ± 0.0010
2^+_2	2-ph	0.00065 ± 0.00058	0.00080 ± 0.00070	0.00043 ± 0.00040
0^+_1	2-ph	0.054 ± 0.021	0.056 ± 0.022	0.027 ± 0.010

values of the K and L_1 NMEs in Eqs. (3) and (4) are the same to the accuracy given in Table I so that only one value of the NME is given for the β^+/EC and ECEC modes. In Table I the mean values and standard deviations of the NMEs were computed from the set of four NMEs; namely, the normal and hybrid NMEs (see the explanation below) for the extreme values $g_{\rm A} = 1.00$ and $g_{\rm A} = 1.25$ of the axial-vector coupling constant.

In computing the NMEs of Table I and the corresponding half-lives of Fig. 2 the adjusted single-particle basis was used with the ranges $g_{\rm A} = 1.00$–1.25 and $g_{\rm pp} = 0.80$–1.05. In addition to using the standard expression for the $2\nu2\beta$ NME [see Eq. (10) of [21]] also a "hybrid" expression for the NME was used. In the hybrid NME the computed value of the transition amplitude corresponding to the lowest second leg $^{78}{\rm Br}(1^+_{\rm gs}) \to {}^{78}{\rm Se}(J^+_f)$ of the $2\nu2\beta$ transition amplitude was replaced by the corresponding experimental value for each of the final states $J^+_f = 0^+_{\rm gs}, 2^+_1, 2^+_2, 0^+_1$. The experimental amplitudes were extracted from the experimental log ft values of the corresponding Gamow-Teller transitions in Fig. 1, as is done in the single-state-dominance approximation (see, e.g., Refs. [44,45]). Unfortunately, for the extraction of the amplitude of the lowest first-leg transition $^{78}{\rm Kr}(0^+_{\rm gs}) \to {}^{78}{\rm Br}(1^+_{\rm gs})$ there is no experimental data on the corresponding β^- transition $^{78}{\rm Br}(1^+_{\rm gs}) \to {}^{78}{\rm Kr}(0^+_{\rm gs})$. Hence, the amplitude had to be extracted from the corresponding log ft value in a similar system of initial and final nuclei. As this "sister" transition the adjacent β^- transition $^{80}{\rm Br}(1^+_{\rm gs}) \to {}^{80}{\rm Kr}(0^+_{\rm gs})$ could be used, with the log ft value log $ft = 5.5$.

It is interesting to note from Table I that for the 0^+ final states the ECEC and β^+EC NMEs are approximately a factor of 2 larger than the $\beta^+\beta^+$ NMEs. In fact, the ECEC NMEs are exactly two times the $\beta^+\beta^+$ NMEs. This is easy to understand when looking at the construction of the NMEs in Eq. (9) of Ref. [21]. The energy denominators of the $\beta^+\beta^+$ NMEs and ECEC NMEs are given in Eqs. (13) and (17) of Ref. [21], respectively. When the approximation $\varepsilon_{{\rm b}i} \approx 1$ is used in Eq. (20) of Ref. [21], then the energy denominator of the ECEC NMEs in Eq. (17) of Ref. [21] is exactly half the energy denominator of the $\beta^+\beta^+$ NMEs in Eq. (13) of Ref. [21]. For the β^+EC NMEs the approximation $\varepsilon_{{\rm b}i} \approx 1$ does not lead to such an exact relation as in the previous case but to something that is close.

The value of the axial-vector coupling constant $g_{\rm A}$ strongly affects the magnitudes of the phase-space factors $G^{\alpha}_{2\nu}(I^+)$ in Eqs. (2)–(4) since it appears there in the fourth power. In the present calculations this dependence of the phase-space factors does not overwhelm the dependence of the NME on $g_{\rm pp}$, however. This means that the lower (upper) limits of the half-lives in Fig. 2 correspond to $g_{\rm A} = 1.00$ ($g_{\rm A} = 1.25$). The situation in the corresponding decays of ^{96}Ru in Ref. [21] was the opposite and the main uncertainty there stemmed from the uncertainty in the energy of the first excited 1^+ state in the intermediate nucleus ^{96}Tc.

It is well visible in Fig. 2 that the half-lives corresponding to the 2^+ final states are much longer than those corresponding to the 0^+ final states; the reason for this being that the related NMEs are much smaller for the 2^+ final states, as witnessed in Table I. This feature was already noticed in the early work of Ref. [15]. Concerning the detection possibilities of the $2\nu2\beta$ processes in ^{78}Kr, the best chances of detection in the near future offer the ECEC and β^+EC decays to the ground state with the computed half-lives in the range of $(9$–$44) \times 10^{21}$ years. The best experimental limit thus far for the ground-state-to-ground-state double K-capture mode has been set to $T^{\rm EC(K)EC(K)}_{2\nu}(0^+_{\rm gs}) \geqslant 2.3 \times 10^{20}$ yr in Ref. [46] and for the β^+EC(K) mode to $T^{\beta^+{\rm EC(K)}}_{2\nu}(0^+_{\rm gs}) \geqslant 1.1 \times 10^{20}$ yr in Ref. [47]. These half-life limits are still almost two orders of magnitude below the presently computed ones but maybe not so far for the experiments exploiting modern technologies like the ultralow-background HPGe γ spectrometry [48]. Based on the computed results it is clear that the detection of the decays to the 2^+ final states is hopeless in the foreseeable future.

C. Neutrinoless modes of double-β decays

Let us next discuss the observables related to $0\nu2\beta$ decays. As discussed in Sec. III the adopted range of values for the particle-particle parameter is $g_{\rm pp} = 0.80$–1.05. The calculated Jastrow- and UCOM-correlated NMEs for the $0\nu2\beta$ decays of interest are shown in Table II. In Table II the first column lists the NMEs for the two different final states in ^{78}Se; namely, the ground state and the first excited 0^+ state 0^+_1 at 1498.60 keV of excitation, presumed to be a two-phonon state. The values of the Gamow-Teller, Fermi, and total NMEs have been given for both Jastrow and UCOM short-range correlations and the two extreme values of the axial-vector coupling constant.

From Table II one observes that the UCOM-correlated NMEs are larger than the Jastrow-correlated ones for the ground-state transition, but not too much difference is seen for

TABLE II. Computed Jastrow and UCOM correlated NMEs for the ground-state and excited-state decays of ^{78}Kr. The 0_1^+ state is described as a coupling of two 2_1^+ ccQRPA phonons.

NME	Jastrow		UCOM	
	$g_A = 1.00$	$g_A = 1.25$	$g_A = 1.00$	$g_A = 1.25$
$M_{GT}^{(0\nu)}(0_{gs}^+)$	5.750	3.271	7.091	4.438
$M_{F}^{(0\nu)}(0_{gs}^+)$	− 2.368	− 0.331	− 2.796	− 0.716
$M^{(0\nu)'}(0_{gs}^+)$	5.196	3.482	6.328	4.896
$M_{GT}^{(0\nu)}(0_1^+)$	0.052	0.039	0.037	0.054
$M_{F}^{(0\nu)}(0_1^+)$	− 0.120	− 0.008	− 0.120	− 0.009
$M^{(0\nu)'}(0_1^+)$	0.110	0.044	0.100	0.059

the 0_1^+ state, interpreted as a two-phonon state. Similar patterns were observed for the corresponding transitions in the case of the ^{96}Ru decay in Ref. [21]. The key to the different behaviors of the two transitions are the different decompositions of the NMEs in terms of the total angular momentum of the decaying protons: for the ground-state transition this decomposition is dominated by the monopole $J' = 0$ pairs while for the two-phonon transition there is no dominating component in the J' decomposition as seen in Fig. 4 of Ref. [21]. There is also a large difference between the NMEs computed for the two extreme values of g_A. This is based on the two extreme values of $g_{pp} = 0.80$ and $g_{pp} = 1.05$ used in the two calculations. In these calculations the correspondence between g_{pp} and g_A has been taken such that increasing g_A corresponds to increasing g_{pp}. This is in line with the characteristics of the two-neutrino $\beta^-\beta^-$ decay to the ground state for which the same correlation between g_A and g_{pp} prevails due to the decrease of the pnQRPA computed NME with increasing g_{pp} and the similar decrease of the experimental NME with increasing g_A. If the experimental and computed NMEs were to correspond to each other, then increasing g_A would automatically lead to an increasing value of g_{pp}. Also for the positron-decaying nuclei, like ^{78}Kr, a similar correspondence between g_A and g_{pp} realizes for the two-neutrino modes.

The NMEs of Table II can be combined with the appropriate phase-space factors to produce predicted half-lives for a given value of the effective neutrino mass $\langle m_\nu \rangle$. The half-lives of the discussed $0\nu2\beta$ modes can be cast in the form

$$T_{1/2}^{\beta^+\beta^+} = T_0^{\beta^+\beta^+}(\langle m_\nu\rangle[\text{eV}])^{-2}, \quad (12)$$

$$T_{1/2}^{\beta^+\text{EC}} = T_0^{\beta^+\text{EC}}(\langle m_\nu\rangle[\text{eV}])^{-2}, \quad (13)$$

TABLE III. Auxiliary factors of Eqs. (12) and (13) for the decays of ^{78}Kr.

State	s.r.c.	T_0	
		$\beta^+\beta^+$	β^+EC
0_{gs}^+	UCOM	$(9.42 - 15.7) \times 10^{26}$	$(3.90 - 6.51) \times 10^{26}$
	Jastrow	$(1.40 - 3.11) \times 10^{27}$	$(5.78 - 12.9) \times 10^{26}$
0_{2-ph}^+	UCOM		$(1.66 - 4.79) \times 10^{31}$
	Jastrow		$(1.39 - 8.66) \times 10^{31}$

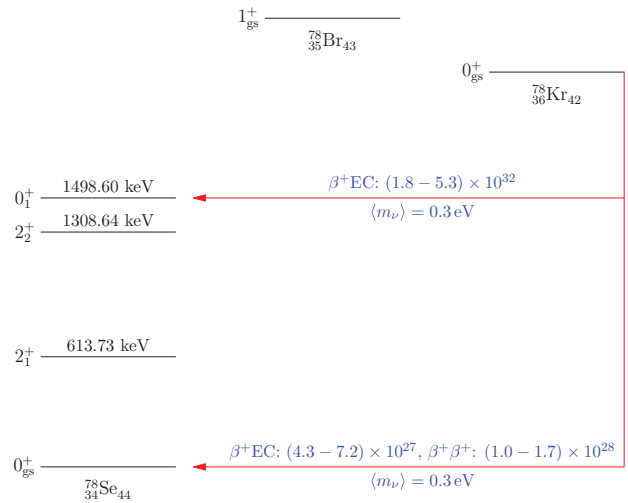

FIG. 3. (Color online) Computed partial decay half-lives of β^+EC and $\beta^+\beta^+$ decay transitions from the ground state of ^{78}Kr to the ground state and first-excited 0^+ state in ^{78}Se. The UCOM short-range correlations are used and the half-lives are given in units of years for the effective neutrino mass $\langle m_\nu \rangle = 0.3$ eV.

where the effective neutrino mass should be inserted in units of eV. In Table III the auxiliary factors of the above equations are given for both the Jastrow and UCOM short-range correlations. The UCOM correlated NMEs are used in Fig. 3 to display the decay half-lives (12) and (13) for the effective neutrino mass $\langle m_\nu \rangle = 0.3$ eV.

From Table III and Fig. 3 one observes that for the decays to the ground state the half-lives are in the range of 10^{27}–10^{28} years. For the decay to the 0_1^+ state the half-lives are in the range of 10^{32} years and thus most likely undetectable.

V. SUMMARY AND CONCLUSIONS

The possible modes of the two-neutrino and neutrinoless double-beta decays of ^{78}Kr have been studied and the associated nuclear matrix elements and decay half-lives have been computed. A QRPA-based theory framework with G-matrix-based two-body interactions and realistically large single-particle bases have been used in the calculations. The computed values of the nuclear matrix elements and the corresponding half-lives have been tabulated for two different short-range correlations. Complementary information about the half-lives has been displayed in figures.

The two-neutrino ECEC and β^+EC double-beta decays to the ground state have computed half-lives in the range of 10^{22} years and thus are potentially detectable in (near) future experiments. The range of half-lives for the neutrinoless double-beta decays starts from about 10^{28} years for effective neutrino masses of few tenths of eV.

ACKNOWLEDGMENTS

This work was supported by the Academy of Finland under the Finnish Center of Excellence Program 2012-2017 (Nuclear and Accelerator Based Program at JYFL).

[1] M. Doi, T. Kotani, and E. Takasugi, Prog. Theor. Phys. Suppl. **83**, 1 (1985).
[2] J. Suhonen and O. Civitarese, Phys. Rep. **300**, 123 (1998).
[3] F. T. Avignone III, S. R. Elliott, and J. Engel, Rev. Mod. Phys. **80**, 481 (2008).
[4] A. S. Barabash, Phys. Rev. C **81**, 035501 (2010).
[5] M. Doi and T. Kotani, Prog. Theor. Phys. **87**, 1207 (1992).
[6] M. Doi and T. Kotani, Prog. Theor. Phys. **89**, 139 (1993).
[7] J. Bernabeu, A. De Rujula, and C. Jarlskog, Nucl. Phys. B **223**, 15 (1983).
[8] S. Rahaman, V. Elomaa, T. Eronen, J. Hakala, A. Jokinen, J. Julin, A. Kankainen, A. Saastamoinen, J. Suhonen, C. Weber, and J. Äystö, Phys. Lett. B **662**, 111 (2008).
[9] M. I. Krivoruchenko, F. Šimkovic, D. Frekers, and A. Faessler, Nucl. Phys. A **859**, 140 (2011).
[10] J. Suhonen, Eur. Phys. J. A **48**, 51 (2012).
[11] J. Suhonen, J. Phys.: Conf. Series **375**, 042026 (2012).
[12] J. Suhonen and O. Civitarese, J. Phys. G **39**, 085105 (2012).
[13] J. Suhonen, Phys. Rev. C **48**, 574 (1993).
[14] M. Hirsch, K. Muto, T. Oda, and H. Klapdor-Kleingrothaus, Z. Phys. A: Hadrons Nucl. **347**, 151 (1994).
[15] M. Aunola and J. Suhonen, Nucl. Phys. A **602**, 133 (1996).
[16] M. Aunola and J. Suhonen, Nucl. Phys. A **643**, 207 (1998).
[17] J. Suhonen and M. Aunola, Nucl. Phys. A **723**, 271 (2003).
[18] V. Kolhinen, V. Elomaa, T. Eronen, J. Hakala, A. Jokinen, M. Kortelainen, J. Suhonen, and J. Äystö, Phys. Lett. B **684**, 17 (2010).
[19] V. S. Kolhinen, T. Eronen, D. Gorelov, J. Hakala, A. Jokinen, A. Kankainen, J. Rissanen, J. Suhonen, and J. Äystö, Phys. Lett. B **697**, 116 (2011).
[20] J. Suhonen, Phys. Lett. B **701**, 490 (2011).
[21] J. Suhonen, Phys. Rev. C **86**, 024301 (2012).
[22] J. Suhonen and O. Civitarese, Nucl. Phys. A **847**, 207 (2010).
[23] J. Suhonen, Int. J. Mod. Phys. E **20**, 451 (2011).
[24] J. Suhonen, Nucl. Phys. A **853**, 36 (2011).
[25] J. Suhonen, *From Nucleons to Nucleus: Concepts of Microscopic Nuclear Theory* (Springer, Berlin, 2007).
[26] J. Suhonen, Nucl. Phys. A **563**, 205 (1993).
[27] O. Civitarese and J. Suhonen, Nucl. Phys. A **575**, 251 (1994).
[28] G. A. Miller and J. E. Spencer, Ann. Phys. (NY) **100**, 562 (1976).
[29] H. Feldmeier, T. Neff, R. Roth, and J. Schnack, Nucl. Phys. A **632**, 61 (1998).
[30] M. Kortelainen, O. Civitarese, J. Suhonen, and J. Toivanen, Phys. Lett. B **647**, 128 (2007).
[31] M. Kortelainen and J. Suhonen, Phys. Rev. C **75**, 051303(R) (2007).
[32] M. Kortelainen and J. Suhonen, Phys. Rev. C **76**, 024315 (2007).
[33] J. Suhonen and M. Kortelainen, Int. J. Mod. Phys. E **17**, 1 (2008).
[34] F. Šimkovic, A. Faessler, V. Rodin, P. Vogel, and J. Engel, Phys. Rev. C **77**, 045503 (2008).
[35] J. Suhonen, Nucl. Phys. A **864**, 63 (2011).
[36] J. Menéndez, A. Poves, E. Caurier, and F. Nowacki, Nucl. Phys. A **818**, 139 (2009).
[37] T. R. Rodríguez and G. Martínez-Pinedo, Phys. Rev. Lett. **105**, 252503 (2010).
[38] J. Barea, J. Kotila, and F. Iachello, Phys. Rev. C **87**, 014315 (2013).
[39] F. Šimkovic, G. Pantis, J. D. Vergados, and A. Faessler, Phys. Rev. C **60**, 055502 (1999).
[40] A. Bohr and B. R. Mottelson, *Nuclear Structure* (Benjamin, New York, 1969), Vol 1.
[41] J. Suhonen and O. Civitarese, J. Phys. G **39**, 124005 (2012).
[42] J. Suhonen, T. Taigel, and A. Faessler, Nucl. Phys A **486**, 91 (1988).
[43] J. Suhonen, Phys. Lett. B **607**, 87 (2005).
[44] O. Civitarese and J. Suhonen, Phys. Rev. C **58**, 1535 (1998).
[45] O. Civitarese and J. Suhonen, Nucl. Phys. A **653**, 321 (1999).
[46] J. M. Gavriljuk, V. V. Kuzminov, N. Y. Osetrova, and S. S. Ratkevich, Phys. At. Nucl. **63**, 2297 (2000).
[47] C. Sáenz *et al.*, Phys. Rev. C **50**, 1170 (1994).
[48] P. Belli, R. Bernabei, F. Cappella, R. Cerulli, F. A. Danevich, S. d'Angelo, A. Incicchitti, M. Laubenstain, O. G. Polischuk, D. Prosperi, and V. I. Tretyak, Eur. Phys. J. A **42**, 171 (2009).